ACCELERATOR EXPERIMENTS ON THE CONTRIBUTION OF SECONDARY PARTICLES TO THE PRODUCTION OF COSMOGENIC NUCLIDES IN METEORITES

P.Dragovitsch and P.Englert
Department of Nuclear Chemistry, University of Köln,
D-5000 Köln 1, FRG

R.Michel
ZfS, University of Hannover, D-3000 Hannover 1, FRG

1. Introduction. Through the interaction of galactic cosmic particle radiation (GCR) a wide variety of cosmogenic nuclides is produced in meteorites. They provide valuable historical information about both the cosmic radiation and the bombarded meteorites. An important way to understand the production mechanisms of cosmogenic nuclides in meteorites is to gather information about the depth and size dependence of the build-up of GCR-secondary particles within meteorites of different sizes and chemical compositions. This can be obtained by analyzing cosmogenic nuclide depth profiles in meteorites [e.g. 1]. However, suitable meteorites are rare and the especially significant short-lived radioactive species have not been measured extensively. Simulation experiments with meteorite models offer an alternative to direct observation providing a data basis to describe the development and action of the secondary cascade induced by the GCR in meteorites.

2. Methods. A series of thick target irradiations of spherical meteorite models with radii (R) of 5, 15 and 25cm with 600 MeV protons, the maximum of the differential GCR proton fluxes, was performed at the CERN-synchrocyclotron [2]. The materials used to simulate the meteorite body were diorite (R=5cm) and gabbro (R=15,25cm), both having a density of $\sim$3g cm^{-3} and an extremely low water content of $\leq 10^{-3}$g/g. Pure elemental foils and simple chemical compounds were exposed to the particle fields along cores drilled perpendicular to each other through the center of the models. A homogeneous 4π isotropic irradiation was achieved combining four independent movements (two translational and two rotational) of the meteorite models in the fixed particle beam. The irradiation parameters for the three simulation experiments are given in table 1.

Table 1: Irradiation parameters of the 600 MeV proton simulation experiments

Model-radius [cm]	Irrad.time [min]	p-Dose [cm^{-2}]	"Exposure age" [10^6y]
5	489.5	4.82×10^{15}	76.0
15	750.0	2.17×10^{14}	3.4
25	763.0	5.99×10^{14}	9.3

3. Results and discussion. The depth-dependent production rates of radionuclides and stable isotopes from the target elements were determined by gamma spectroscopy, low-level counting techniques, accelerator- and conventional mass

spectrometry. The symbols in Figures 1a-e show the experimental production rates of five short-lived radioactive products in units of [10^{-4} atoms $s^{-1}g^{-1}$] as a function of depth within the meteorite models, assuming a primary proton flux of [$1cm^{-2}$ s^{-1}]. Product nuclides and targets are given in the Figures. The limits of uncertainty do not exceed the size of the symbols unless indicated by error bars. Figures 1a-e show only a small fraction of over 90 target-product-pairs obtained or in the process of reduction for each of the meteorite models. This selection especially emphasizes low energy secondary reactions. The extreme examples are the $^{27}Al(n,\alpha)^{24}Na$-reaction and the (n,p)-reaction on ^{54}Fe, mainly responsible for the ^{54}Mn production from iron. The other reactions occur at slightly higher threshold energies such as the $^{59}Co(n,2n)^{58}Co$ reaction, the mainly proton induced $^{27}Al(p,3p4n)^{22}Na$ reaction and the exclusively proton induced reaction $^{56}Fe(p,n)^{56}Co$.

Focussing on the measured data points in Figure 1, it is obvious that the depth profiles of all these low energy products increase from the surface to the center by 20%-30% independent of the radius of the meteorite model. This behavior was expected for the R=15cm and the R=25cm spherical model, but was striking for the R=5cm model, demonstrating that the contribution of GCR-secondaries cannot be neglected in small meteorites.

It is also remarkable that for all of the mainly neutron-produced species, the absolute production rates at the centers of the model meteorites increase with increasing model-radius, as predicted for low-energy secondary products in meteorites by various model calculations [3,4].For the exclusively proton produced $^{56}Co(Fe)$, the center activities for the two large meteorite models are indistinguishable within the limits of uncertainty. Moreover, for the ^{22}Na-production from Al, the highest center activity is found in the R=15cm model, whereas the center activity of the largest sphere is only slightly higher than that of the smallest. Taking into consideration that the production rates of the $^{56}Fe(p,n)^{56}Co$-reaction are more than an order of magnitude lower than those of the others the reversal of the sequence for ^{22}Na may then only be attributed to lower fluxes of charged secondaries above the threshold energy at the center of the largest model.

More precise information about the action of low energy secondary hadrons within the meteorite models can be obtained by calculating the contributions of primary protons to the production of the nuclides. The solid lines in Figure 1 show the calculated primary proton-induced contributions. The calculations consider stopping and absorption of the primaries, their fluxes for given energies and given positions [5] and excitation functions of the individual nuclear reactions[6]. The general tendency for cosmogenic nuclide production by primary protons is a decrease in production rate from the surface to the center. For the small R=5cm sphere the absolute contribution of secondary neutrons increases with increasing

threshold and charge (Z) of the target from the $^{27}Al(n,\alpha)$ over the $^{54}Fe(n,p)$ to the $^{58}Co(n,2n)$ reaction, i.e. the primary contribution becomes less important. For other nuclear reactions in all models a systematic description of the primary and secondary contribution as a simple function of Z of target, threshold energy and model radius cannot be observed. It is necessary to study the nuclear parameters of each individual target-product pair in detail. Nevertheless, the depth profiles presented provide an excellent basis for a quantitative description of primary and secondary particle fields in extended spherical targets under proton bombardment.

A more general point of interest is the question as to whether the 600 MeV simulation experiments performed are suitable to interpret observations in meteorites. There are several obstacles that prevent a direct comparison of the depth profiles in Figure 1 with meteorite data. Short-lived radionuclides have been measured only in a limited number of meteorite falls. Depth profiles of short-lived isotopes in meteorites have not been determined. Table 2 lists a number of meteorites of different preatmospheric sizes for which a few short-lived isotopes were measured [7]. Their production rates are given in the same units as in Figure 1. In view of these limitations the following conclusions can be made: ^{54}Mn and ^{22}Na-production rates follow directly the tendency given in Figure 1: they increase from the smallest to the largest meteorites. Assuming an average Fe-concentration of 25%, the respective production rates in table 2 will have to be multiplied by a factor of 4 to be directly comparable. In case of the ^{54}Mn-production in meteorites, Fe is the major target and the meteorite production rate thus exceeds the one found in the models by a factor of 3-4. The same is valid to a larger extent for the ^{22}Na-production, but here the largest contribution in a meteorite comes from Mg. The slight differences between actual meteorite data and the results of the simulation series presented may be caused by the use of diorite and gabbro to develop the secondary cascade, the density and average Z of which is somewhat lower than that of most meteorite classes; another reason may be found in using 600 MeV protons only.

Though the results of the 600 MeV proton irradiation series look very promising in modeling GCR primary and secondary fluxes in meteorites, further experiments using higher energies and different particles are necessary to more accurately simulate realistic conditions in space.

4. Acknowledgement. This work was partially funded by the DFG.

References: [1] P.Englert and W.Herr (1980), Earth Planet. Sci.Lett. 47 361-369. [2] R.Michel et al. (1984), Lun.Planet. Sci. XV, 542-543. [3] R.Reedy (1985), J.Geophys.Res. 90, C722-C728. [4] T.P.Kohmann and M.L.Bender (1967), in: B.S.P.Shen (ed.) High Energy Nuclear Reactions in Astrophysics, Benjamin, N.Y.. [5] R.Michel and R.Stück (1984),J.Geophys.Res. 89 B673-B684. [6] J.Tobailem, C.-H.de Lassus St. Genies (1975), CEA-N-1466 (1). [7] J.C. Evans et al. (1982), J.Geophys.Res. 87,

5577-5591. [8] N.Bhandari et al. (1980), Nucl.Tracks 4, 213-262. [9] P.Englert (1985), Lun.Planet.Sci. XVI, 215-216. [10] K.Marti et al. (1969), in: P.Millmann (ed.) Meteorite Research, Reidel, 248-266.

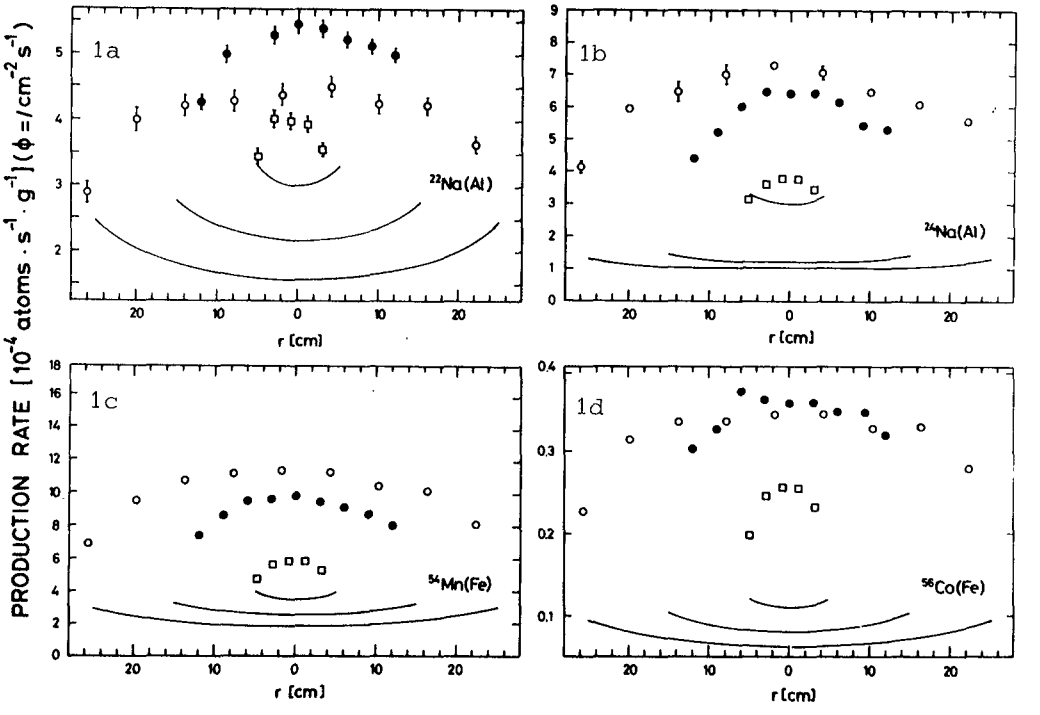

Figures 1a-e: Production rates of short-lived isotopes in meteorite models as a function of depth. A primary proton flux of [1cm^{-2}s^{-1}] is assumed.

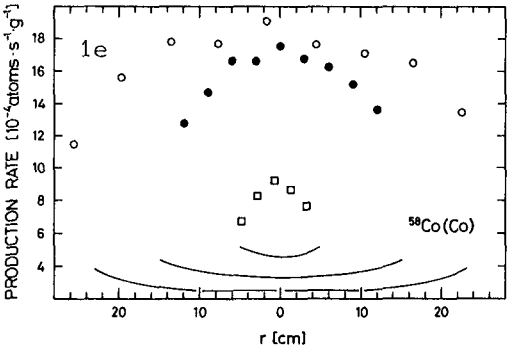

Table 2: Short-lived radionuclides in meteorites of different preatmospheric sizes [7]

Meteorite	Class	Preatm. mass [kg] [8]	Production rates [10^{-4}atoms $s^{-1}g^{-1}$] ^{22}Na	^{54}Mn
Denver	L6	1.35	5.74±0.16	6.50±1.70
Murchison	CM2	>15	6.75±0.25	6.40±0.33
Lost City	H5	<200 [9]	5.67±0.16	5.33±0.25
St.Severin	LL6	372±14	8.41±0.66 [10]	6.75±0.16 [10]
Innisfree	L	350±100	7.92±0.41	6.92±0.33
Dhajala	H3	850±135	9.08±0.16	13.16±0.50
Jilin	H	>3000	9.50±0.41	11.30±1.50